Hydrological Research Letters **18**(4), 111–116 (2024)
Published online in J-STAGE (www.jstage.jst.go.jp/browse/hrl). DOI: 10.3178/hrl.18.111

Evaluation of rainfall prediction in the vicinity of Solomon Islands with a high-resolution non-hydrostatic model

Kosuke Ito[1] and Edward Maru[1,2,3]
[1]*Disaster Prevention Research Institute, Kyoto University, Japan*
[2]*Forecasting Section, Solomon Islands Meteorological Service, Solomon Islands*
[3]*Graduate School of Engineering and Science, University of the Ryukyus, Japan*

Abstract:

Meteorological authorities in many developing countries can benefit from running a regional model optimized for their countries in addition to rainfall predictions provided by major centers in developed countries. As one such activity, Solomon Islands Meteorological Services (SIMS) recently started to operationally run their regional model based on the non-hydrostatic model of Japan Meteorological Agency (JMA). This study evaluates the skill of rainfall predictions by the SIMS operational model with a 15-km mesh (SI15) based on 219 cases of 36-hour forecasts initialized every five days during 2017–2019. We also conducted runs with a 1.875-km mesh (SI01) in anticipation of future numerical resources. The skill was compared with the forecasts of the JMA Global Spectral Model (GSM), using rain gauge data and satellite-based data. The forecasts by SI15 and SI01 exhibited better performance than the GSM in terms of bias and threat score, with SI01 performing the best. Additionally, SI01 successfully reproduced the diurnal variation where precipitation becomes strong over land in the evening and on the eastern side of the Solomon Islands over the sea in the early morning. In contrast, SI15 showed weak biases around the initial time and strong biases after 18 hours of forecast time.

KEYWORDS rainfall prediction; operational system; nonhydrostatic model

INTRODUCTION

Rainfall is closely related to daily life and water resources, and heavy rain can cause disasters such as floods and landslides. Thus, the improvement of rainfall prediction is vitally important for society. Although the performance of rainfall predictions has been improving year by year, meteorological authorities in many developing countries rely on global weather prediction models with a 10–20 km mesh from major centers such as the Japan Meteorological Agency (JMA), European Centre for Medium-Range Weather Forecasts, and United States National Centers for Environmental Prediction. One potential issue is that a global model may not be sufficient to resolve local-scale convective activities. With recent economic development and the availability of non-hydrostatic models, it is becoming increasingly feasible for meteorological authorities in developing countries to conduct high-resolution regional atmospheric model simulations specialized for their country. This can be a good strategy for improving the forecast skill of rainfall.

The Solomon Islands Meteorological Service (SIMS) is one such meteorological authority located in the Solomon Islands, an island nation consisting of six major islands and over 900 smaller islands in the South Pacific, with average annual rainfall ranging from 2,400 to 4,800 mm. The Solomon Islands often experience intense rainfall events leading to disasters (Deo *et al.*, 2021), and the occurrence rate of malaria depends on the rainfall amount in the region (Smith *et al.*, 2017).

Toward improving predictions, SIMS received permission from the JMA on 10 July 2018 to use the JMA's non-hydrostatic model (NHM), and a prediction system with a 15 km mesh commenced operational use on 4 August 2020. It provides daily forecasts of rainfall, surface wind direction, and wind speed once a day from 12UTC.

The SIMS refers to the outputs from this system based on their experience. However, there has been no quantitative evaluation of whether the system is useful compared with global models. Therefore, the first aim of this study is to assess the performance of rainfall prediction by the system. Additionally, under the assumption that more computational resources would become available in the future, numerical experiments were also conducted with a 1.875 km mesh to discuss the advantages of such a high-resolution model. This work is useful for ensuring the benefits and limitations of the current operational system, and planning for future systems. The findings are valuable for other developing countries which may consider operating a similar regional model.

METHODS

In this study, we use the NHM (Saito, 2012), employing two horizontal grid spacings of 15 km and 1.875 km. Hereafter, numerical simulations using the 15 km mesh are called SI15, while those using the 1.875 km mesh are called

Correspondence to: Kosuke Ito, Severe Storm and Extreme Weather, Disaster Prevention Research Institute, Kyoto University, S-504D, Gokasho, Uji, Kyoto 611-0011, Japan. E-mail: ito.kosuke.2i@kyoto-u.ac.jp

Received 4 June, 2024
Accepted 11 August, 2024
Published online 27 November, 2024

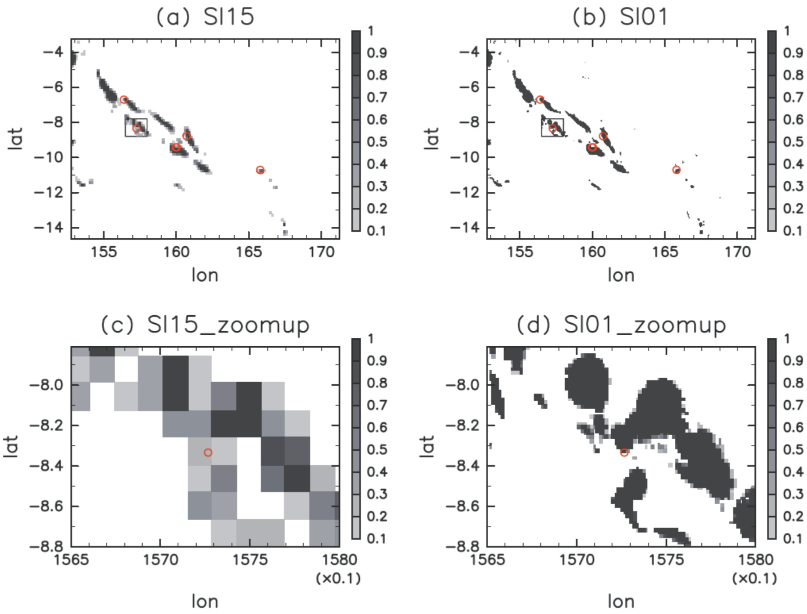

Figure 1. (a–b) Land and sea ratio of grids. Red circles indicate the manned rain gauge stations. (c–d) Same as (a–b) but for the limited area indicated by the black rectangles in (a–b)

SI01. The model physics of SI15 are the same as in the SIMS operational model. Both models employ 6-category bulk microphysics. SI15 employs the modified Kain-Fritsch scheme for cumulus parameterization (Kain and Fritsch, 1990), while SI01 does not use cumulus parameterization. As a boundary layer scheme, both use the Mellor-Yamada-Nakanishi-Niino level-3 closure model (Nakanishi and Niino, 2004).

The forecast time (FT) was up to 36 hours, conducted at 5-day intervals from 12UTC on 1 January 2017 to 12UTC on 27 December 2019. In total, the number of simulations was 219 for each experiment. For presentation purposes, the FT of XX hours is written as FTXX, and the period of FT from XX to YY hours is written as FTXX–YY. The computational domain covers an area of 2250 km × 1500 km centered at 9.0°S and 162.0°E, encompassing the entire Solomon Islands. Initial and boundary conditions are the forecast outputs of the JMA's global spectrum model (GSM) provided at 0.5° spacings in both latitude and longitude, while GSM has an approximately 20 km mesh. Initial vertical motion and the mixing ratio of clouds and rain are assumed to be zero. The GSM outputs were also used for evaluating the rainfall forecast skill of the global model.

The topographic data employs Global 30 Arc-Second Elevation, which has a resolution of approximately 1 km. Figure 1 illustrates the land-sea ratio (a portion of land in each grid) for SI15 and SI01. When the land-sea ratio within a grid cell is between 0 and 1, the physical property of the cell is intermediate between sea and land. Major islands are well represented even in SI15. Upon closer inspection, smaller islands and complex coastlines are not well represented in SI15 compared to SI01 (see Figure 1c–d). The use of a high-resolution model is expected to better resolve the sea-land contrast, which impacts on sea breezes and convection.

The forecast quality of rainfall events over 219 simulations was evaluated using the bias score (BS) and threat score (TS):

Table I. List of six manned stations in Solomon Islands

Province	Station (WMO No.)	Longitude	Latitude
Choiseul	Taro (91502)	156.38°E	6.70°S
Western	Munda (91503)	157.27°E	8.33°S
Malaita	Auki (91507)	160.73°E	8.78°S
Guadalcanal	Honiara (91517)	159.97°E	9.42°S
Guadalcanal	Henderson (91520)	160.05°E	9.42°S
Temotu	Lata (91541)	165.80°E	10.70°S

$$BS = \frac{H + F}{H + M} \tag{1}$$

$$TS = \frac{H}{H + F + M} \tag{2}$$

where H is the number of successful predictions, F is the number of points at which the predicted precipitation corresponds to a false alarm, and M is the number of points at which the observed precipitation was missed by the prediction. BS is the bias in the number of forecasted events relative to the number of observed events. BS is closer to 1.0 if the bias is small. TS means the ratio of the number of correct forecasts relative to the total number of correct forecasts, false alarms, and missed forecasts. A high TS indicates better forecast skill, where TS = 1 means a perfect forecast.

As a reference, in-situ daily precipitation measurements from 00UTC to 00UTC by rain gauges at six manned stations (Table I and Figure 1; Note that Henderson and Honiara are located very closely) were taken from the archived records in SIMS. The number of observations used to evaluate the corresponding rainfall forecast skill was 1263 (219 runs multiplied by six stations; 51 missing data). To check the diurnal variation, we also used 3-hourly accumulated rainfall from the same six stations archived in the integrated surface database (ISD; Smith *et al.*, 2011). Since GSM forecasts are available with a 6-hour interval, we first constructed 6-hourly accumulated rainfall data by the sum of two successive 3-hour accumulated rainfall data. The rate of missing data for 6-hourly accumulated rainfall was high (47%) because at least one of two successive 3-hourly accumulated rainfall data was not transferred to the Global Telecommunication System (GTS), on which ISD 3-hourly data relies in this region, particularly at night. We also used hourly satellite-based precipitation data from the Global Satellite Mapping of Precipitation (GSMaP) moving vector with a Kalman filter v8.0 (Kubota *et al.*, 2020) to check the rainfall in the broader area. We used the delayed mode version without correction by rain gauges. Although GSMaP is powerful for remotely obtaining hourly rainfall in a broad area, the 0.1° mesh is not sufficient to fully resolve the impact of small islands, and the quality of GSMaP is limited by the frequency of satellite observations and its algorithm.

RESULTS

Daily rainfall prediction

Figure 2a–b shows the *BS* and *TS* of daily rainfall predictions averaged over all samples from the six stations. The evaluation was conducted for 24-hour accumulated rainfall (00-00 Coordinated Universal Time (UTC)), which corresponds to FT12–36 of numerical models. The *x*-axis refers to the lower limit of 24-hour accumulated rainfall (for example, "$2{\cdot}10^1$" means >20 mm/day).

Generally, the *BS* of the numerical models was larger than one, indicating an overestimation of the frequency of precipitation events. The GSM excessively overestimated the frequency with accumulated rainfall of less than 10 mm/day. By contrast, fewer strong rainfall events of more than 50 mm/day were predicted by GSM. *BS* in SI15 and SI01 were larger than one but closer to one compared to GSM. Particularly, SI01 exhibits the best *BS* among the three models. In SI15, *BS* tended to be higher with increasing accumulated rainfall. This cautions that there is a higher probability of false alarms predicted by the current SIMS operational model for strong rainfall, and this issue would be alleviated by a high-resolution model.

The *TS* decreased as precipitation intensity increased in all forecast models, reflecting that more intense precipitation events are harder to predict. Compared with GSM, SI15 and SI01 yielded better prediction skill for rainfall. Furthermore, SI01 generally yielded higher *TS* than SI15, indicating its higher prediction skill. The correlation coefficient for precipitation amounts against rain gauges was 0.303 in SI01, 0.252 in SI15, and 0.150 in GSM. It is encouraging to see the better skill of the current SIMS operational model in comparison with GSM, and further improvements with a high-resolution model.

In the above-mentioned evaluation, model grid points closest to the rain gauge locations were used. Because the spatial representativeness of SI15 is different from that of SI01, we also calculated the rainfall amount averaged over 8 × 8 grid points in SI01, occupying the same area represented by a single grid of SI15. The area-averaged rainfall amount was referred to as SI01_ave. The *BS* in SI01_ave was more positively biased than in SI01 for rainfall of 10 mm/day or less. However, *BS* in SI01_ave was closer to one in comparison with SI15. The *TS* in SI01_ave was highest, with the highest correlation coefficient against rain gauges (0.341). Small-scale details in the forecast are less reliable, but areal averages might be useful to not miss the potential for rainfall.

Diurnal variation

Diurnal cycles are an important variation for rainfall in the tropics (Janowiak *et al.*, 1994; Yang and Slingo, 2001). Oceanic deep convection tends to reach its maximum in the early morning, while convection over land generally peaks in the evening (e.g. Yang and Slingo, 2001). We evaluated the forecast skills of diurnal rainfall characteristics using 6-hour accumulated rainfall (Figure 3). Note that FT0–6, FT6–12, FT12–18, FT18–24, FT24–30, and FT30–36 correspond to 12–18 UTC (23–05 LST), 18–00 UTC (05–11 Local Standard Time (LST)), 00–06 UTC (11–17 LST), and 06–12 UTC (17–23 LST), respectively. Figure 3a shows that the GSM yielded excessive rainfall predictions regardless of FTs. NHM-based models are better than GSM in terms of *BS*. The *BS* in SI01 and SI01_ave was much closer to one, while SI15 overestimated weak precipitation events in the later FTs. On the other hand, NHM-based

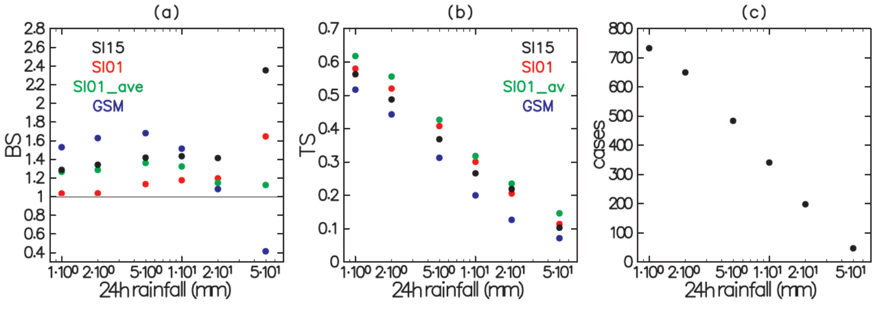

Figure 2. (a) Bias score and (b) threat score from SI15, SI01, SI01_ave, and GSM categorized by the daily rainfall amount. (c) The number of samples for each category

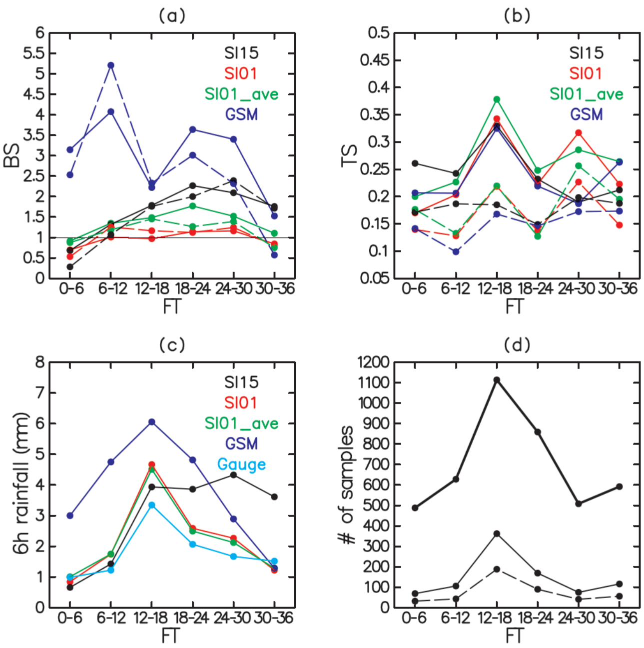

Figure 3. (a) Bias score and (b) threat score based on predictions from SI15, SI01, SI01_ave, and GSM categorized by the forecast time (FT). Solid lines are for accumulated rainfall of >1 mm/6 h, while broken lines are for accumulated rainfall of >5 mm/6 h. (c) Sample-mean 6-hourly accumulated rainfall from rain gauges and forecast models. (d) A thin solid line represents the number of samples exceeding 1 mm of 6-hourly rainfall for each FT, while a thin broken line represents the number of samples exceeding 5 mm of 6-hourly rainfall. A thick solid line represents the total number of samples

models underestimate the rainfall amount at the earlier FT. This could be attributed to the need for spin-up time for these models because there is no ascending motion and clouds at the initial time in SI15 and SI01.

*TS*s are generally low in GSM and high in SI01 and SI01_ave but depend on the FTs (Figure 3b). Fluctuations might come from an insufficient number of samples. High *TS*s at FT12–18 (11–17 LST) mean that the rainfall prediction in the evening is relatively accurate. SI01 and SI01_ave might be superior to SI15 and GSM at FT24–30, which corresponds to 23–05 LST, although we need to caution around the small number of samples for precipitations from night to early morning (Figure 3d). The sample-mean 6-hour accumulated rainfall is clearly strong in the evening and weak at night to early morning, consistent with previous studies. SI01 and SI01_ave could quantitatively reproduce this observed diurnal variation throughout the FTs (Figure 3c). In contrast, SI15 overestimated the rainfall amount after FT18, as GSM did throughout the FTs except at FT30–36.

To confirm the sea-land contrast, the mean 6-hourly accumulated rainfall in GSMaP is shown during 12–18 UTC (23–05 LST), 18–00 UTC (05–11 LST), 00–06 UTC (11–17 LST), and 06–12 UTC (17–23 LST) in Figure 4. The results are generally consistent with previous studies, in that the mean precipitation over the ocean peaks in the early morning, particularly in the eastern sea of the Solomon Islands, while that over land peaks in the evening. Upon closer inspection, the eastern sea of the Solomon Islands had stronger rainfall than the western sea in the early morning. This can be explained by interaction with the background easterly trade wind (Aoki and Shige, 2024; Du and Rotunno, 2018).

The comparison with model predictions indicates that the rainfall amount in SI15 and SI01 is weaker at FT0–6, while that in SI15 becomes excessive after FT18 (Figure 4). Regarding the diurnal variation, all models (GSM, SI15, and SI01) could reproduce strong (weak) precipitation over the ocean (islands) in the early morning, with maximum precipitation occurring over the eastern seas of the Solomon Islands. They also represent strong precipitation over the islands in the evening. One notable difference is that the contrast of rainfall amount between land and sea was smaller in GSM and larger in SI01. Particularly, precipitation over land was greater in SI01 in the evening. This result does not entirely align with GSMaP results. Considering that SI01 reasonably captures the diurnal variation in in-situ observations (Figure 3c), the rainfall amount in SI01 may not be so excessive over land. In fact, the correlation and root-mean-squared difference of daily rainfall between GSMaP and rain gauges was 0.576 and 16.65 mm, respectively. It might come from insufficient GSMaP quality or improper reproductivity in NHM-based models. While GSMaP is valuable to monitor the near-real-time rainfall amount, its limitations should be recognized.

Figure 5 depicts the mean 6-hourly rainfall amounts between FT12–18 from SI15 and SI01 along with the topography, focusing on a limited area. In SI01, strong rainfall was generally observed along the terrain, including strong precipitation near 157.0°E, 8.0°S. This is an interesting topic to be validated with dense observations in the future.

CONCLUDING REMARKS

While meteorological authorities in many developing countries use precipitation predictions from global models operated by developed countries, it has become more feasible for them to operate their weather forecast systems thanks to recent economic development and the availability of non-hydrostatic models. As one of these authorities, the Solomon Islands Meteorological Service (SIMS) started to run a numerical forecast model based on the Japan Meteorological Agency Non-hydrostatic model (NHM) since 2018. This study aimed to evaluate the forecast skill for rainfall with a 15-km mesh model (SI15), equivalent to the current SIMS operational model, against the global spectral model (GSM). Additionally, a finer 1.875-km mesh model (SI01) was evaluated toward future development. The verification was based on 219 runs of 36-hour forecasts.

SI15 was demonstrated to be superior to GSM in terms of threat score and bias score. The forecast skill of SI01 was further improved over that of SI15, particularly in reducing the false alarms of heavy rain. It was also found that rainfall averaged over 8 × 8 grid points in SI01 improved the threat score.

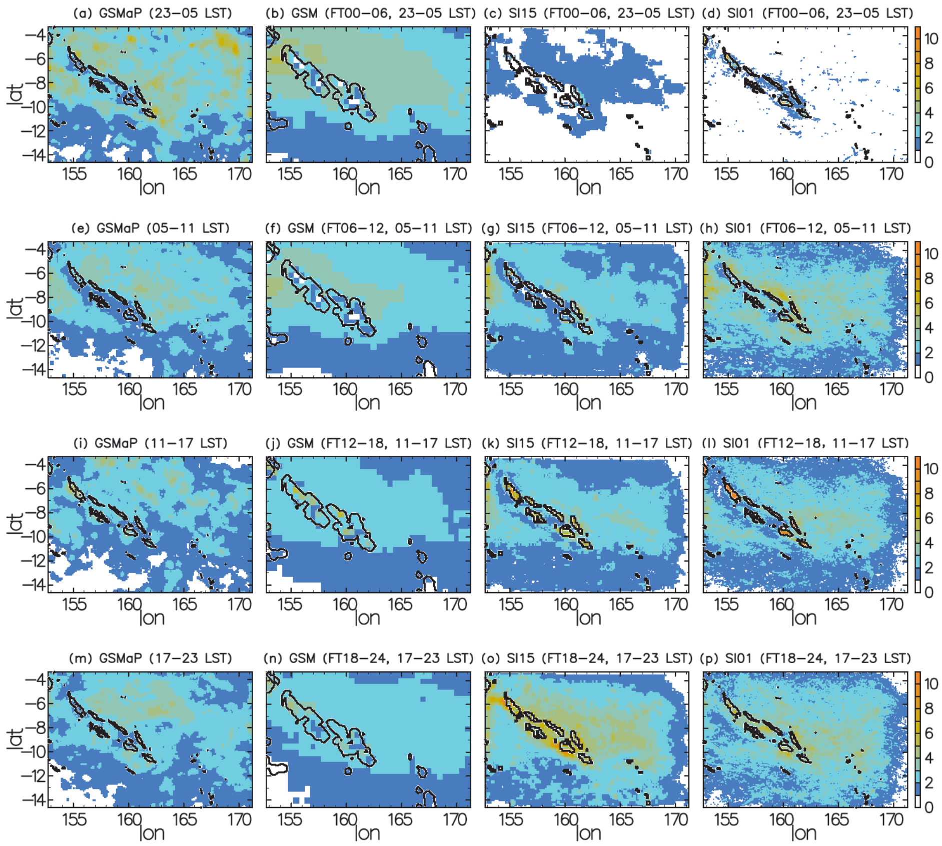

Figure 4. Mean 6-hourly rainfall amount. Each column corresponds to GSMaP analysis and forecasts from GSM, SI15, and SI01 from left to right, respectively. The forecast results are arranged from top to bottom in six-hour intervals during FT0–6 (23–05 local standard time (LST)), FT6–12 (05–11 LST), FT12–18 (11–17 LST), and FT18–24 (17–23 LST), in which the period of forecast time from XX to YY hours is written as FTXX–YY

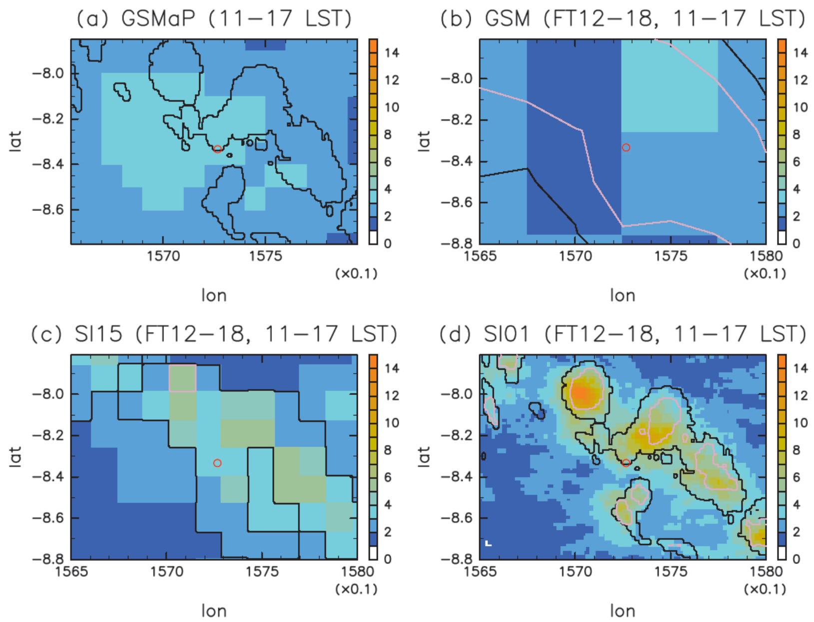

Figure 5. Mean 6-hourly rainfall amount in 11–17 local standard time (LST) for a limited region from (a) GSMaP. (b–d) Corresponding rainfall amount between forecast time (FT) of 12–18 h in (b) GSM, (c) SI15, and (d) SI01. A red circle indicates the location of a rain gauge in Munda. (c–d) Black contours indicate grids with the land ratio of more than 10%, and magenta contours indicate a height level of 200 m

Although it has been shown that the current operational system (SI15) is beneficial in comparison with the GSM, several biases in SI15 should be kept in mind. From the initial time to the forecast time (FT) up to 6 hours, the rainfall amount has a weak bias, probably due to simulation spin-up. Another issue is that SI15 tends to predict excessive rainfall amounts after FT18. The forecasts in SI01 and SI01_ave successfully reproduced the diurnal variation of rainfall amounts recorded by the rain gauges.

GSMaP observation shows that precipitation on islands tends to be higher during the day, with increased precipitation in the early morning over the ocean, particularly on the eastern sea of the Solomon Islands. The contrast in precipitation between land and sea was consistent with SI01 outputs, presumably due to the high-resolution of topography and coastline. However, the detailed distribution should be further validated with dense in-situ observations in the future.

The current experiments spanning three years demonstrate the benefits and cautions for SIMS in having their own regional non-hydrostatic models rather than relying solely on global models. Of course, it is insufficient to address the impact of long-term features such as global warming, El Niño-Southern Oscillation (ENSO), and monsoons. Indeed, rainfall in the Solomon Islands is highly correlated with the ENSO cycle, and the amount of rainfall could increase by double during La Niña relative to El Niño in Guadalcanal (Murphy *et al.*, 2014). Quigley *et al.* (2016) revealed that Honiara's rainfall is driven mostly by the monsoon feeding into the South Pacific Convergence Zone (SPCZ) during the wet season from November to April. During the May to October dry season, the SPCZ weakens as the monsoon and the intertropical convergence zone move northwards. These offer future topics to be investigated with more experiments.

Although much work is needed in the future, this research serves as a first step to ensure the benefits and limitations of employing the current SIMS operational model in comparison with a global model, leading to better daily life, water resource management, and disaster prevention in the Solomon Islands. The study also suggests that the use of a fine-mesh model could further enhance the accuracy of these forecasts. This is feasible when more computational resources become available. In this study, we primarily focused on precipitation prediction in the vicinity of the Solomon Islands; meteorological authorities in other developing countries can employ the same approach to benefit from regional weather models optimized for their country.

ACKNOWLEDGMENTS

This paper is based on achievements of the collaborative research program (2024WS-03) of the Disaster Prevention Research Institute of Kyoto University. This work was supported by JSPS KAKENHI Grant JP23K17804, and the Program for The Advanced Studies of Climate Change Projection (SENTAN, Grant Number JPMXD0722678534) funded by MEXT.

REFERENCES

Aoki S, Shige S. 2024. Control of low-level wind on the diurnal cycle of tropical coastal precipitation. *Journal of Climate* **37**: 229–247. DOI: 10.1175/JCLI-D-23-0180.1.

Deo A, Chand SS, Ramsay H, Holbrook NJ, McGree S, Magee A, Bell S, Titimaea M, Haruhiru A, Malsale P, Mulitalo S, Daphne A, Prakash B, Vainikolo V, Koshiba S. 2021. Tropical cyclone contribution to extreme rainfall over southwest Pacific Island nations. *Climate Dynamics* **56**: 3967–3993. DOI: 10.1007/s00382-021-05680-5.

Du Y, Rotunno R. 2018. Diurnal cycle of rainfall and winds near the south coast of China. *Journal of the Atmospheric Sciences* **75**: 2065–2082. DOI: 10.1175/JAS-D-17-0397.1.

Janowiak JE, Arkin PA, Morrissey M. 1994. An examination of the diurnal cycle in oceanic tropical rainfall using satellite and in situ data. *Monthly Weather Review* **122**: 2296–2311. DOI: 10.1175/1520-0493(1994)122<2296:AEOTDC>2.0.CO;2.

Kain JS, Fritsch JM. 1990. A one-dimensional entraining/detraining plume model and its application in convective parameterization. *Journal of the Atmospheric Sciences* **47**: 2784–2802. DOI: 10.1175/1520-0469(1990)047<2784:AODEPM>2.0.CO;2.

Kubota T, Aonashi K, Ushio T, Shige S, Takayabu YN, Kachi M, Arai Y, Tashima T, Masaki T, Kawamoto N, Mega T, Yamamoto MK, Hamada A, Yamaji M, Liu G, Oki R. 2020. Global Satellite Mapping of Precipitation (GSMaP) products in the GPM era. *Advances in Global Change Research* **67**: 355–373. DOI: 10.1007/978-3-030-24568-9_20.

Murphy BF, Power SB, McGree S. 2014. The varied impacts of El Niño–Southern Oscillation on Pacific island climates. *Journal of Climate* **27**: 4015–4036. DOI: 10.1175/JCLI-D-13-00130.1.

Nakanishi M, Niino H. 2004. An improved Mellor–Yamada level-3 model with condensation physics: its design and verification. *Boundary-Layer Meteorology* **112**: 1–31. DOI: 10.1023/B:BOUN.0000020164.04146.98.

Quigley N, Beavis SG, White I. 2016. Rainwater harvesting augmentation of domestic water supply in Honiara, Solomon Islands. *Australian Journal of Water Resources* **20**: 65–77. DOI: 10.1080/13241583.2016.1173314.

Saito K. 2012. The JMA Nonhydrostatic model and its applications to operation and research. *Atmospheric Model Applications* 85–110. DOI: 10.5772/35368.

Smith A, Lott N, Vose R. 2011. The integrated surface database: recent developments and partnerships. *Bulletin of the American Meteorological Society* **92**: 704–708. DOI: 10.1175/2011BAMS3015.1.

Smith J, Tahani L, Bobogare A, Bugoro H, Otto F, Fafale G, Hiriasa D, Kazazic A, Beard G, Amjadali A, Jeanne I. 2017. Malaria early warning tool: linking inter-annual climate and malaria variability in northern Guadalcanal, Solomon Islands. *Malaria Journal* **16**: 472. DOI: 10.1186/s12936-017-2120-5.

Yang G-Y, Slingo J. 2001. The diurnal cycle in the tropics. *Monthly Weather Review* **129**: 784–801. DOI: 10.1175/1520-0493(2001)129<0784:TDCITT>2.0.CO;2.